

Investigation of the Spring Thermal Bar Phenomenon Based on Mathematical and Laboratory Modeling

D. A. Solov'ev^a and R. I. Nigmatulin^b

Presented by Academician R.F. Ganiev February 26, 2010

Received March 2, 2010

DOI: 10.1134/S1028334X10100120

The regularities of the appearance and development of large-scale ordered convective motions and natural currents, which are the essence of the thermal bar phenomenon, are studied on basis of the mathematical and physical (laboratory) modeling. Joint application of these two methods allows us to compensate for the lack of exact exhaustive mathematical description of this phenomenon, which is cumbersome and requires a large amount of the initial data that are difficult to obtain. The main objective of our research is to gain the physical similarity between the phenomena observed in the model conditions and the whole class of the investigated phenomena.

Recently, the degree of technogenic anthropogenic impact on the aquatic environment has become a global problem that is particularly topical in the conditions of the possible variations in the global climate and requires urgent solution. The quality of water in the rivers, lakes, and reservoirs used for drinking water supply is gradually decreasing. Successful solution of this problem requires investigation of the processes responsible for the redistribution of water masses [1]. Convective mixing is related to the processes determining unique properties of water mixing in fresh water reservoirs and formation of its thermal balance. In the spring and autumn periods, special attention should be focused on the convection related to the anomalous dependence of water density on temperature near 4°C. The formation of a thermal bar (or, briefly, a thermobar, originating from French *barre*, which is an obstacle) is exclusively related to the temperature of the maximum water density. Such a tem-

perature for salinities less than 24.7°C is above the freezing point. As a result, during the spring warming and autumnal cooling of waters, the surface waters pass the point of maximum density. The appearance of convective water motion leads to the formation of a vertical boundary (thermal bar) along the 4°C isotherm with intense lowering of waters separating the coastal zone of the lake from the internal part. During these seasons, thermohydrodynamic processes related to the development of the thermal bar are the main factors determining the peculiarities of water mixing, which are responsible for the water quality. Therefore, one has to take into account the contribution of phenomenon such as the thermal bar to the ecological state of the water reservoir and the dynamics of its development when developing practical plans of nature preservation in water basins. A more complete account of this contribution requires comprehensive investigation of the thermal bar, which would allow us to consider the influence of a wide spectrum of possible mechanisms determining the thermal state and dynamics of its development considering a variety of weather conditions. Such an approach opens wide possibilities to develop a more realistic model of this natural phenomenon. In our work, we performed theoretical and experimental analysis of the dynamics of the development of the thermal bar.

The objective of this work is to study the thermal bar dynamics by means of numerical experiments and laboratory modeling with account for the influence of wind, solar irradiance, and fluxes of latent and sensible heat.

The mathematical model is a development of the model elaborated earlier [2–4]. The model considers the motion of an incompressible viscid fluid under the influence of the gravity field in a domain whose sizes correspond to the sizes of the laboratory setup tank. The problem was solved in the Cartesian coordinate system Ox_1, Ox_2, Ox_3 .

^a Shirshov Institute of Oceanology, Russian Academy of Sciences, Nakhimovskii pr. 36, Moscow, 117997 Russia

^b Scientific Center for Nonlinear Wave Mechanics and Technology, Russian Academy of Sciences, ul. Bardina 4, Moscow, 119991 Russia
e-mail: solovev@sail.msk.ru

The system of the Navier-Stokes equations in the Boussinesq approximation is used to describe the thermohydrodynamic processes (equation of thermal conductivity and equation of state for fresh water) written with account for the methods of distinguishing large-scale structures in a turbulent medium [5]. The equation of state included the quadratic dependence of the water density on temperature near 4°C. Following [5] we write the final equation system in the variables of the stream function ψ and vorticity φ :

$$\frac{\partial U_1}{\partial t} + \frac{\partial \psi}{\partial x_3} \frac{\partial U_1}{\partial x_2} - \frac{\partial \psi}{\partial x_2} \frac{\partial U_1}{\partial x_3} - 2 \frac{\partial \psi}{\partial x_3} \Omega \sin \alpha = \mu \left(\frac{\partial^2 U_1}{\partial x_2^2} + \frac{\partial^2 U_1}{\partial x_3^2} \right), \quad (1)$$

$$\frac{\partial \varphi}{\partial t} + \left(\frac{\partial \psi}{\partial x_3} \frac{\partial \varphi}{\partial x_2} - \frac{\partial \psi}{\partial x_2} \frac{\partial \varphi}{\partial x_3} \right) + 2 \frac{\partial U_1}{\partial x_3} \Omega \sin \alpha = \mu \left(\frac{\partial^2 \varphi}{\partial x_2^2} + \frac{\partial^2 \varphi}{\partial x_3^2} \right) - 2(T - T_4) \frac{\partial T}{\partial x_2}, \quad (2)$$

$$\frac{\partial T}{\partial t} + \left(\frac{\partial \psi}{\partial x_3} \frac{\partial T}{\partial x_2} - \frac{\partial \psi}{\partial x_2} \frac{\partial T}{\partial x_3} \right) = \mu \left(\frac{\partial^2 T}{\partial x_2^2} + \frac{\partial^2 T}{\partial x_3^2} \right), \quad (3)$$

$$\Delta \psi = \varphi, \quad (4)$$

where, U_1 , U_2 , and U_3 are velocities along the corresponding coordinate axes x_1 , x_2 , x_3 ; α is the geographical latitude; and Ω is the angular velocity of the Earth's rotation. Equation system (1)–(4) is written in the dimensionless form, where the following normalizing units were accepted: depth of the basin H for the distances; $\sqrt{\frac{1}{\gamma}}$ for temperature; \sqrt{gH} for velocity; $\sqrt{\frac{H}{g}}$ for time; $\mu = \frac{\nu_T}{H\sqrt{gH}}$ is a dimensionless coefficient of turbulent viscosity; T and T_4 are dimensionless values of the temperature and the temperature of the maximum freshwater density. Here, $\gamma = 0.75 \times 10^{-5} \text{ }^\circ\text{C}^{-2}$, ν_T is the coefficient of turbulent viscosity, and g is acceleration due to gravity.

We shall use the coefficient of turbulent viscosity to close the equation system (1)–(4), which we also reduce to the dimensionless form taking into account the introduced units of measure. Finally, we get

$$\mu^2 = \left(\frac{\nu_T}{H\sqrt{gH}} \right)^2 = \frac{c^3}{S} \int \left[4 \left(\frac{\partial^2 \psi}{\partial x_2 \partial x_3} \right)^2 + \left(\frac{\partial^2 \psi}{\partial x_3^2} - \frac{\partial^2 \psi}{\partial x_2^2} \right)^2 ds - (T - T_4) \frac{\partial T}{\partial x_3} \right] ds, \quad (5)$$

where S is the dimensionless square of the domain for the problem solution.

The boundary conditions were specified as follows. The free surface condition was specified at the upper boundary: the wind stress along axis x_2 and the variable heat flux as a function of the time of the day, which includes the radiance and balance heat flux Q_R and the latent Q_L and sensible Q_T heat fluxes between the water basin and the atmosphere. The directions of Q_L and Q_T can be either positive or negative depending on the initial conditions of the numerical model.

The nonslip condition, zero transport condition for velocity, and zero heat fluxes were specified at the bottom of the basin, and for the left and right inclined lateral boundaries. The temperature distribution field corresponding to the conditions of the experiment and the zero velocity field was specified as the initial condition.

The solution of equation system (1)–(4) with the equation of closure (5) and the boundary and initial conditions was realized using the method of alternating directions (implicit scheme) [6]. The problem was solved on a grid with 1800 nodes.

The “Thermobar-1” laboratory setup is a rectangular glass tank with length $l = 1.5$ m and width $s = 0.4$ m [7, 8]. The tank basin in the longitudinal direction is sloping; and its angle α can be varied from 0° to 15°. The water that fills the tank with a fixed bottom slope forms a wedge. In order to prevent heat transport through the bottom and walls, they were thermally isolated by foam plastic. Heat flux Q at the water surface was determined with five electric lamps ranging from 40 to 210 W/m². The water temperature was measured with four vertical profilers with attached temperature sensors.

The wind generator consisting of two ventilators with a diameter of 0.2 m was used to induce wind circulation in the laboratory tank. The velocity of the air flow induced by ventilators was measured with an electronic anemometer in the range from 0 to 5 m/s.

In the laboratory experiments, the inclination of the tank bottom to the horizontal was set at 6° and the water depth was 0.16 m. The radiation flux in the laboratory experiment was 210 W/m², which did not differ much from the typical values in the natural conditions in spring [9]. The main portion of heat from the incandescent lamps was absorbed by the top centimeter of the water layer in the tank. According to the corresponding vertical proportions of the laboratory and real water basin, the model simulated absorption of the solar heat in the few uppermost meters of the lake.

Before the beginning of each experiment, the tank was filled with tap water and ice. During melting of ice, the water temperature decreased to $T_0 < T_m$ ($T_m = 4^\circ\text{C}$). The water in the basin was mixed to equalize the temperature inhomogeneities, and before warming the water was left at rest for a few minutes. The measurements were carried out along the longitudinal section

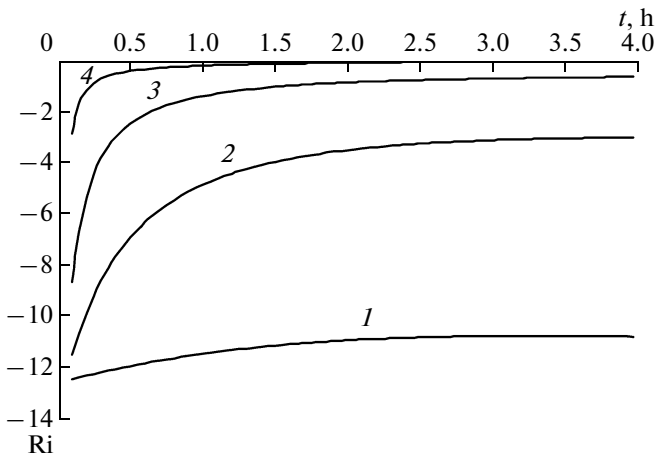


Fig. 1. Dependence of the Richardson number on the time of wind forcing of various intensity. Wind velocity: $V = 2$ (1), 4 (2), 6 (3), 10 m/s (4).

at the middle of the basin. The air flow induced by the wind generator was directed parallel to the water surface. The wind forcing was oriented in two-coordinate directions along the free surface of water in the tank.

The circulation structure of currents at different wind velocities was revealed as a result of numerical and laboratory experiments. The range of critical values of wind velocity was found, at which the drift current forms a zone of water mass convergence, which does not coincide with the 4°C isotherm and suppresses density convection preventing the formation of the thermal bar. An increase in the wind velocity leads to suppressing of thermal convection. It is accompanied by an increase in the velocity of the fluid circulation. This is confirmed by the Richardson number

$$Ri = \frac{\Delta\rho g l}{\rho V^2}$$

which determines the role of thermal stratification in the vertical energy transport in comparison with the dynamic factors, which include wind forcing at the surface of the reservoir. If the Richardson number is much less than unity, the buoyancy force does not play a significant role for the current. If it is greater than unity, the buoyancy force dominates. Figure 1 presents the dependence of the differential

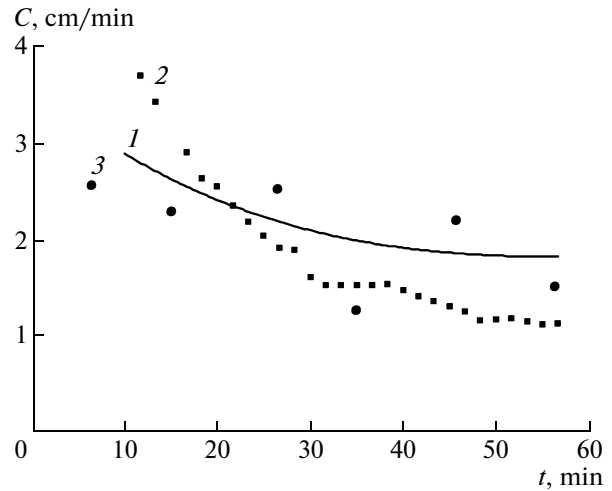


Fig. 2. Velocity C of thermal bar displacement: (1) numerical calculation; (2) laboratory experiment; (3) normalized AVHRR Pathfinder satellite data for Lake Ladoga (direction SSE–NNW) during the period from May 1 to June 31, 2008.

Richardson number on the time of the wind forcing in the model reservoir.

When wind velocity increases, the Richardson number approaches zero, which illustrates the dominating role of the inertia forces over the buoyancy force. The time dependence of the Richardson number can facilitate estimating the time duration of the reconstruction of currents until they reach the stationary state in the entire region of the modeled reservoir under constant wind velocity. Reconstruction and formation of the stationary regime occurs more slowly under weak wind (Fig. 1, curves 1, 2) compared with the case of significant wind forcing, which reconstruct the current during a few tens of minutes (Fig. 1, curves 3, 4).

A rapid motion of the 4°C isotherm at the water surface under weak wind forcing from the coast and its slow motion under wind forcing in the direction of shallow water despite its slow motion in the central part of the reservoir were found in both cases in the series of laboratory experiments. This result indicates that a nonlinear dependence of heat advection on the direction and intensity of wind exists between the

External parameters and measured characteristics of the thermal bar

Study object	Data	$\tan\alpha$	$Q, \text{W/m}^2$	$T_0, \text{°C}$	$\Delta l, \text{m}$	$\Delta t, \text{s}$	$\langle Tw \rangle, \text{°C}$
Lake Ontario	[10]	3×10^{-3}	250	2	11×10^3	84×10^4	4.9
Lake Ladoga	[9]	2×10^{-3}	167	0	17×10^3	198×10^4	6.4
Numerical calculation	[4]	1×10^{-1}	210	0	1.4	24×10^2	5.2
Laboratory experiments	[11]	9×10^{-2}	376	0	1.21	39×10^2	6.2
	[8]	1×10^{-1}	10	0	1.4	24×10^2	4.8

warm and cool parts of the reservoir. A comparison of the displacement velocity of the thermal bar with the satellite IR-observations (AVHRR Pathfinder) in Lake Ladoga during the period from May 1 to June 31, 2008, is shown in Fig. 2. The data of field observations were normalized with the account for the spatiotemporal scales model—field experiment. The comparison was performed by scaling of the lake size provided that the similarity is maintained by the Froude and Taylor numbers.

The mean velocities of the thermal bar displacement based on the calculation data, experiments, and satellite AVHRR Pathfinder observations were 2.15, 1.8, and 34.7 cm/min, respectively. The discrepancy between the calculation and experimental data is likely related to the peculiarities of the thermal regime of the reservoir in each specific case.

During the numerical experiment, the values of fluxes Q_T , Q_L , and their total value Q_Σ were estimated on the basis of transport equations [9] at different values of the wind velocity. The values of these fluxes were calculated for the difference between the air and water temperatures ranging from -10 to $+10^\circ\text{C}$ at constant relative air humidity 60%. Figure 3 demonstrates the situation characteristic of the spring period when the air temperature insignificantly exceeds the water surface temperature in the modeled reservoir. In this case, the total heat flux is directed to the atmosphere, which is related to the excess of the latent heat over the sensible heat.

The opposite situation is also possible when the sensible heat flux is dominating. In this case, the joint action of both fluxes directed to the reservoir would lead to additional warming of the surface waters, and hence, to the increase in the velocity of thermal bar displacement. It follows from the calculations that the account for these fluxes in the boundary conditions is significant in the numerical models simulating natural reservoirs. According to our estimates, this can lead to a variation in the velocities of the convective density currents ranging from 20 to 25% proportionally to the additional heat transported to the water column. Due to nonuniform warming of the surface waters in the coastal and deep parts of the reservoir, the direction of the total latent and sensible heat fluxes can have different signs at the surface of the reservoir. In the deep part of the reservoir, surface waters are additionally warmed (due to the large difference between the air and water temperatures), while in the coastal region, the water is cooled (due to the smaller difference between the air and water temperatures).

The characteristics of the thermal bar measured during the work agree satisfactory with the data of other authors presented in table prepared on the basis of the papers cited most frequently. The table presents the external parameters determining the development of the thermal bar: $\tan\alpha$ is the tangent of the bottom slope, Q is heat flux through the water surface, and T_0 is

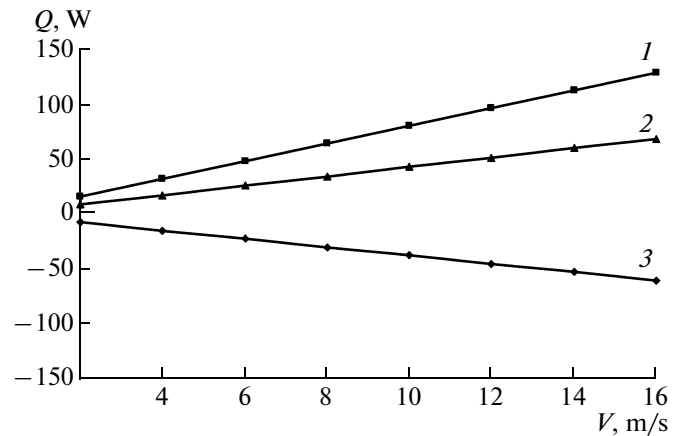


Fig. 3. Dependence of heat fluxes between the reservoir and atmosphere on the wind forcing for the case when the air temperature exceeds the surface water temperature in the modeled reservoir by 2°C . (1) Latent heat flux Q_L ; (2) total heat flux $Q_\Sigma = Q_L + Q_T$; (3) sensible heat flux Q_T .

the initial temperature. The table also presents the characteristics of the thermal bar: Δl is the distance passed by the thermal bar during time Δt ; $\langle Tw \rangle$ is the mean temperature of the warm region by time moment Δt .

The experiments demonstrated that the methods used in the work can be successfully applied to reproduce the characteristic peculiarities of the thermal structure of the reservoir when the water temperature passes the value corresponding to its maximum density in different environmental conditions of the modeled reservoir. The possibility to vary the initial and boundary conditions in the course of the experiment opens new perspectives for further research of the thermohydrodynamic processes using the methods of mathematical and laboratory modeling.

REFERENCES

1. K. V. Pokazeev and N. N. Filatov, *Hydrophysics and Ecology of Lakes* (Mosk. Gos. Univ., Moscow, 2002) [in Russian].
2. N. S. Blokhina and D. A. Solov'ev, *Vestn. Mosk. Univ., Ser. 3, Fizika, Astron.*, No. 3, 59–63 (2006).
3. R. I. Nigmatulin, N. S. Blokhina, and D. A. Solov'ev, *State and Perspectives of Joint Integration of Production and Achievements in Mechanics*, in: *Sbornik Nauchnykh Trudov, Posvyashchennyi Pamyati Akademika Kh.A. Rakhmatulina*, Uzbekistan: Karshi, 7–16 (2003).
4. D. A. Solov'ev, *The Role of Heat and Moisture Exchange between Reservoirs and the Atmosphere in the Thermal Balance of the Reservoir at Different Hydrometeorological Situations. Physical Problems of Ecology (Physical Ecology)* (Maks Press, Moscow, 2010) [in Russian].
5. V. A. Kovalev and A. E. Ordanovich, *A Physico-Mathematical Model of a Turbulent Horizontally Stratified Flow with the Account for Coherent Structures*, Dep. VINITI (Moscow, 1981) [in Russian].

6. P. J. Roache, *Computational Fluid Dynamics* (Hermosa, Albuquerque, 1972; Mir, Moscow, 1980).
7. D. A. Solov'ev, in *Materialy XII mezhdunarod. Symp. "Dinamicheskie i tekhnologicheskie problemy mekhaniki konstruktsii i sploshnykh sred. Izbrannye doklady. Yaropolets, February 13–17, 2006, Moscow, MAI, February 20–22, 2006* (Moscow, 2006), pp. 138–141 [in Russian].
8. D. A. Solovyev, Laboratory-Scale Model of the Spring Thermal Bar Fluxes and Structures in Fluid. Abstr. Intern. Conf. St. Peterburg, 25–26 (2007).
9. A. I. Tikhomirov, *Thermal Properties of Large Lakes* (Nauka, Leningrad, 1982) [in Russian].
10. G. K. Rodgers, "Heat Advection within Lake Ontario in Spring and Surface Water Transparency Associated with the Thermal Bar," Proc. XI Conf. Great Lakes Res. Wisconsin: Univ. Wisconsin-Milwaukee, 480–486 (1968).
11. G. H. Elliott, A Laboratory and Mathematical Study of the Thermal Bar. Ph.D thesis. Vancouver: Inst. Oceanogr., Univ. British Columbia, 189 (1970).